Drought and flood characteristics in the farming-pastoral ecotone of northern China based on the Standardized Precipitation Index

CAO Huicong[1,2*], YAN Dandan[3], JU Yuelin[2]

[1] Journal Department, Nanjing Forestry University, Nanjing 210037, China;
[2] Faculty of Humanities & Social Sciences, Nanjing Forestry University, Nanjing 210037, China;
[3] College of Biology and the Environment, Nanjing Forestry University, Nanjing 210037, China

Abstract: The farming-pastoral ecotone of northern China (FPENC) provides an important ecological barrier which restrains the invasion of desert into Northwest China. Studying drought and flood characteristics in the FPENC can provide scientific support and practical basis for the protection of the FPENC. Based on monthly precipitation data from 115 meteorological stations, we determined the changes in climate and the temporal and spatial variations of drought and flood occurrence in the FPENC during 1960–2020 using the Standardized Precipitation Index (SPI), Morlet wavelet transform, and inverse distance weighted interpolation method. Annual precipitation in the FPENC showed a slightly increasing trend from 1960 to 2020, with an increasing rate of about 1.15 mm/a. The interannual SPI exhibited obvious fluctuations, showing an overall non-significant upward trend (increasing rate of 0.02/a). Therefore, the study area showed a wetting trend in recent years. Drought and flood disasters mainly occurred on an interannual change cycle of 2–6 and 9–17 a, respectively. In the future, a tendency towards drought can be expected in the FPENC. The temporal and spatial distribution of drought and flood differed in the northwestern, northern, and northeastern segments of the FPENC, and most of the drought and flood disasters occurred in local areas. Severe and extreme drought disasters were concentrated in the northwestern and northeastern segments, and severe and extreme flood disasters were mainly in the northeastern segment. Drought was most frequent in the northwestern segment, the central part of the northeastern segment, and the northern part of the northern segment. Flood was most frequent in the western part of the northwestern segment, the eastern part of the northeastern segment, and the eastern and western parts of the northern segment. The accurate evaluation of the degrees of drought and flood disasters in the FPENC will provide scientific basis for the regional climate study and critical information on which to base decisions regarding environmental protection and socio-economic development in this region.

Keywords: farming-pastoral ecotone of northern China (FPENC); Standardized Precipitation Index (SPI); drought; flood; Morlet wavelet transform

*Corresponding author: CAO Huicong (E-mail: caohuicong@njfu.edu.cn)
Received 2021-08-18; revised 2021-11-05; accepted 2021-11-09

1 Introduction

With the acceleration of global warming, the intensity and frequency of extreme climate events in China have changed significantly, resulting in frequent meteorological disasters such as drought and flood (Yang et al., 2008; Li et al., 2014). Studies have shown that drought and flood disasters are the meteorological disasters that occur most frequently, affect most extensive areas, and exert the greatest impact on crop production; the economic losses caused by drought and flood disasters are far more than other disasters (Gao et al., 2016; Cao et al., 2021). There are many drought and flood disaster evaluation indices currently in wide use, including the Standardized Precipitation Index (SPI), the Palmer Drought Severity Index (PDSI), and the Standardized Precipitation Evapotranspiration Index (SPEI) (Kalisa et al., 2020; Anandharuban and Elango, 2021). Therefore, it is crucial to select the most appropriate index for disaster assessment in regional drought and flood prevention and control.

At present, there are many studies (e.g., Wu et al., 2001; Shahabfar and Eitzinger, 2013; Yu et al., 2019; Zhou et al., 2019; Salehnia et al., 2020; Xu et al., 2020; Elouissi et al., 2021; Li et al., 2021) on the characteristics and impact of drought and flood disasters, with a variety of research methods. The SPI values over different time-scales can be applied to different types of drought and flood events, making SPI the most widely used index, applicable to all climate conditions in practice (Xu et al., 2020). Moreover, the SPI is easy to calculate based on precipitation data, requiring fewer data than other indices. Yu et al. (2019) calculated the SPI at different scales based on precipitation data from 10 meteorological stations in Heilongjiang Province of China during 1953–2015, and showed that precipitation is the main factor influencing drought. Zhou et al. (2019) investigated the temporal and spatial evolution of meteorological drought in the Poyang Lake Basin of China, based on the SPI. Elouissi et al. (2021) used the SPI to analyze the extreme drought and flood disasters at 42 meteorological stations in the Macta Basin, northwestern Algeria, during 1970–2011. Li et al. (2021) discussed the temporal variation, periodic variation, and spatial differentiation characteristics of drought and flood in Northeast Guangdong Province of China using the calculated SPI values and other methods such as wavelet analysis and correlation analysis.

The farming-pastoral ecotone of northern China (FPENC) is located in the transition zone between the semi-humid agricultural areas and the arid and semi-arid pastoral areas in northern China (Gao et al., 2021). The agricultural system varies significantly in the FPENC (Li et al., 2018). Due to its sensitivity to climate change and variations in the impact of human activities, the FPENC has formed a fragile ecosystem. Therefore, the study of drought and flood characteristics based on climate data is essential for agricultural development and the structural adjustment of stockbreeding in the FPENC, and even for the sustainable development of the entire national economy of China. The methods for studying regional drought and flood characteristics are becoming more and more mature, and the SPI provides a widely used and highly applicable way. However, most studies have been conducted on a short time-scale, with few studies on the important agricultural and pastoral areas of the FPENC.

Therefore, this paper used various indices and methods, including the SPI, inverse distance weighted interpolation method, and Morlet wavelet transform analysis to study the temporal characteristics, periodic features, and spatial patterns of drought and flood disasters in the FPENC on a long time-scale. Specifically, this study aims to: (1) study the temporal variation characteristics of drought and flood as well as the cycle fluctuation characteristics in the FPENC; (2) reveal the spatial distribution characteristics of drought and flood in the FPENC; and (3) explore the spatial variation characteristics of drought and flood frequency in the FPENC. The results can not only lay a foundation for the climate change and the temporal and spatial changes of drought and flood disasters in the FPENC, but also provide scientific support and practical

basis for environmental protection, policy development, regional sustainable management in the FPENC.

2 Materials and methods

2.1 Study area

The definition of the boundaries of the FPENC varies according to the requirements of each particular study, but most studies share a broadly common definition of its core area. In this paper, the study area is located between 34°49′–48°32′N and 100°57′–124°43′E (Liu et al., 2018) (Fig. 1), with a total area of about 0.726×10^6 km^2. The study area extends from the southwest of Heilongjiang Province in the north to the east of Qinghai Province in the south, passing through ten provinces (autonomous regions) in the northwest, north, and northeast of China (Heilongjiang, Liaoning, Jilin, Hebei, Shanxi, Shaanxi, Gansu, and Qinghai provinces, as well as Inner Mongolia Autonomous Region and Ningxia Hui Autonomous Region). It lies in the semi-humid continental monsoon climate and typical dry continental climate transition zone. The average annual temperature is 2°C–8°C, and the annual precipitation is 250–500 mm. The elevation of the study area increases from northwest to southeast. Farmland and grassland are their main land use types (Liu et al., 2018; Fang et al., 2020). The northern FPENC is an important ecological barrier, which prevents the invasion of deserts into Northwest China. However, due to the changeable climatic conditions in the region and the impact of untoward human farming activities, the FPENC experiences severe soil erosion and frequent natural disasters.

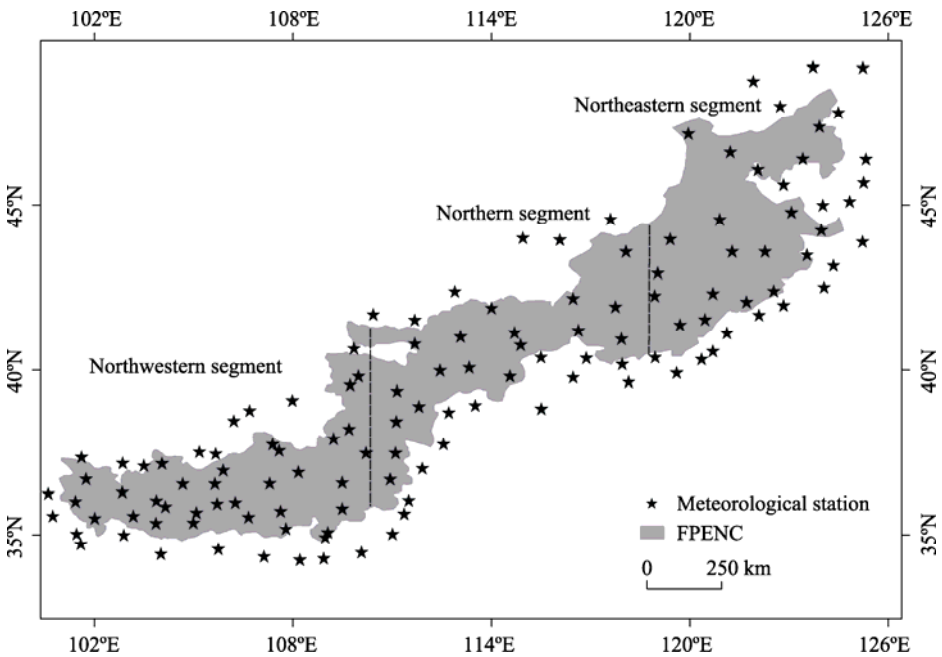

Fig. 1 Overview of the farming-pastoral ecotone of northern China (FPENC). The dotted line divides the FPENC into three parts: northwestern segment, northern segment, and northeastern segment.

2.2 Data sources and processing

The monthly precipitation data for the FPENC during 1960–2020 were obtained from the China Meteorological Data Network (http://data.cma.cn/site/index.html); the distribution of meteorological stations is shown in Figure 1. First, the data from each meteorological station were sorted to ensure their accuracy. In addition, the precipitation data of the stations within and around the study area were strictly screened to eliminate repositioned stations during this period.

Finally, the data from 115 meteorological stations were retained. In order to ensure the integrity and continuity of the data, we performed linear interpolation to estimate the small numbers of missing data, based on the precipitation data for adjacent months at the same station.

2.3 Methods

2.3.1 Standardized Precipitation Index (SPI)

The distribution of precipitation data is usually skewed rather than normal, and the Gamma (Γ) distribution probability is often used to describe changes in precipitation. The SPI can calculate the Γ distribution probability of precipitation over a certain period. A normal standardization can then be performed on the skewed probability distribution, and finally the standardized cumulative precipitation frequency distribution can be used to determine the drought or flood grade (Yu et al., 2019). The steps taken in calculating the SPI are as follows (China Meteorological Administration, 2006).

Assuming that the precipitation in a certain period is a random variable x, then the Γ distribution probability density function ($f(x)$) is shown in the following equation:

$$f(x)=\frac{1}{\beta^{\gamma}\Gamma(x)}x^{\gamma-1}\mathrm{e}^{-\frac{x}{\beta}}\quad(x>0)\,, \tag{1}$$

where e is the natural logarithm; β and γ are the scale and shape parameters, respectively (β>0 and γ>0), which can be obtained by the maximum likelihood estimation method:

$$\hat{\gamma}=\frac{1+\sqrt{1+4A/3}}{4A}, \tag{2}$$

$$\hat{\beta}=\overline{x}/\hat{\gamma}\,, \tag{3}$$

$$A=\log_{10}\overline{x}-\frac{1}{n}\sum_{i=1}^{n}\log_{10}x_i\,, \tag{4}$$

where $\hat{\beta}$ and $\hat{\gamma}$ are the scale and shape parameters, respectively ($\hat{\beta}$>0 and $\hat{\gamma}$>0); A is the intermediate parameter for calculating γ; x_i is the precipitation data sample (mm); $\overline{x}$ is the climate average of precipitation (mm). After determining the parameters in the probability density function, for the precipitation x_0 in a certain year, the probability that the random variable x is less than x_0 can be calculated as:

$$F(x<x_0)=\int_0^{\infty}f(x)\mathrm{d}x\,, \tag{5}$$

where F is the event probability.

The approximate estimate of event probability after substituting Equation 1 into Equation 5 can be calculated by numerical integration.

The event probability when the precipitation is 0.00 mm is estimated by Equation 6:

$$F(x=0)=m/n\,, \tag{6}$$

where m is the number of samples with precipitation of 0.00 mm, and n is the total number of samples.

Normal standardization: the probability values obtained from Equations 5 and 6 are substituted into the standardized normal distribution function (Eq. 7):

$$F(x<x_0)=\frac{1}{\sqrt{2\pi}}\int_0^{\infty}\mathrm{e}^{-Z^2/2}\mathrm{d}x\,, \tag{7}$$

where Z is the SPI.

The SPI can be obtained by approximate solution of Equation 8:

$$\mathrm{SPI}=Z=S\frac{t-(\mathrm{c}_2t+\mathrm{c}_1)t+\mathrm{c}_0}{((\mathrm{d}_3t+\mathrm{d}_2)t+\mathrm{d}_1)t+1.0}, \tag{8}$$

where t is the process parameter during calculation, $t=(\ln(1/F^2))^{1/2}$; and S is the positive and negative coefficient of probability density. If $F>0.5$, then $S=1$; if $F\leq 0.5$, then $S=-1$. In Equation 8, c_0, c_1, c_2, d_1, d_2, and d_3 are constants, with the values of 2.515517, 0.802853, 0.010328, 1.432788, 0.189269, and 0.001308, respectively.

Based on the above method, the SPI values with time-scales of 3-months (SPI-3) and 12-months (SPI-12) were calculated to reflect the seasonal and interannual drought and flood characteristics of the FPENC. In the national standard of classification of meteorological drought (GB/T 20481-2006) (China Meteorological Administration, 2006), the SPI could be divided into different grades of drought and flood (Table 1).

Table 1 Classification standard of drought and flood grades based on the Standardized Precipitation Index (SPI)

Drought/flood grade	SPI
Extreme flood	SPI≥2.0
Severe flood	1.5≤SPI<2.0
Moderate flood	1.0≤SPI<1.5
Light flood	0.5≤SPI<1.0
Normal	–0.5<SPI<0.5
Light drought	–1.0<SPI≤ –0.5
Moderate drought	–1.5<SPI≤ –1.0
Severe drought	–2.0<SPI≤ –1.5
Extreme drought	SPI≤ –2.0

2.3.2 Wavelet transform

One-dimensional complex continuous wavelet analysis was used to extract the various change periods during a time series, in order to fully reflect variations in the trend of the SPI values in different time-scales and estimate the direction of drought and flood trends in the FPENC. The wavelet basis is defined as follows (Teolis, 1998):

$$\varphi(t)=\left(\pi F_{\mathrm{b}}\right)^{-0.5}\times \mathrm{e}^{2i\pi F_{\mathrm{c}}t}\times \mathrm{e}^{-t^2/F_{\mathrm{b}}}, \tag{9}$$

where $\varphi(t)$ is the wavelet function; F_{b} is the bandwidth parameter; e is the natural logarithm; i is the imaginary number; F_{c} is the central frequency; and t is the time (a). Sub-wavelets are generated by stretching and translating the wavelet basis:

$$\varphi_{a,b}(t)=\frac{1}{\sqrt{a}}\varphi\left\{\frac{t-b}{a}\right\}, \tag{10}$$

where $\varphi_{a,b}(t)$ is the sub-wavelet function; a is the scalability factor, and b is the time shift factor.

2.3.3 Drought (or flood) station rate

The drought (or flood) station rate refers to the percentage of weather stations in the study area recording drought (or flood) event in the total stations in the study area. It is used to assess the extent of the influence of drought (or flood). Its calculation follows the formula:

$$P_i=\left(m_i/M\right)\times 100\%, \tag{11}$$

where P_i is the drought (or flood) station rate (%); m_i is the number of weather stations recording drought (or flood) event in the i^{th} year; and M is the total number of weather stations in the study area (115 meteorological stations). The classification criteria for the extent of drought (or flood) are as follows. When drought (or flood) event occurs at most weather stations, i.e., $P_i\geq 70\%$, it is considered drought (or flood) event of the whole region. When $50\%\leq P_i<70\%$, $30\%\leq P_i<50\%$, $10\%\leq P_i<30\%$, and $P_i<10\%$, the extent of drought (or flood) event is considered to be regional drought (or flood), drought (or flood) in partial areas, drought (or flood) in local areas, and no obvious drought (or flood), respectively (Zhang et al., 2015).

2.3.4 Drought (or flood) frequency

The drought (or flood) frequency (Zhang et al., 2015) is used to evaluate the frequency of drought

(or flood) event in the FPENC. Its calculation follows the formula:

$$P_j = \left(n_j / N\right) \times 100\% , \tag{12}$$

where P_j is the drought (or flood) frequency at the j^{th} weather station (%); n_j is the number of years with a certain level of drought (or flood) recorded at the j^{th} weather station; and N is the total number of years studied (61 a in this case).

2.3.5 Inverse distance weighted interpolation

The inverse distance weighted interpolation assumes that each measurement point has a local influence that decreases with increasing distance. Thus, the expression is as follows (Hu et al., 2020):

$$\hat{\mu}(x) = \sum_{i=1}^{n} \omega_i(s) y_i , \tag{13}$$

where $\hat{\mu}(x)$ is the eigenvalue of the interpolation point; $\omega_i(s)$ is the reciprocal of the distance between the sample point and the interpolation point (or the n^{th} power of the reciprocal, where n is a positive integer) function; and y_i is the eigenvalue of the sample point. It should be noted that $\omega_i(s)$ must satisfy the normalization condition:

$$\sum_{i=1}^{n} \omega_i(s) = 1 . \tag{14}$$

After analyzing and correcting the original data, it is found that the distribution of points is uniform and the data density can satisfy the calculation reflecting the changes in the grade of drought (or flood). On this basis, the inverse distance weighted interpolation method was selected for this study.

3 Results

3.1 Characteristics of precipitation change

As shown in Figure 2, the annual precipitation in the FPENC first decreased and then increased during 1960–2020. The average annual precipitation was 445.40 mm, showing only a slight and insignificant increasing trend on the whole (1.15 mm/a). The annual precipitation fluctuated significantly around 1964; the peak value (592.99 mm) occurred in 1964 and the lowest value (346.51 mm) in 1965, with a difference of 246.48 mm. Precipitation was relatively high in the 1960s, when the most extensive fluctuation range was recorded and precipitation values were highly variable. From the 1970s to the 1990s, the annual precipitation fluctuated around the mean value and was relatively stable. Since 2000, the precipitation values have shown an apparent upward trend. Further, the annual precipitation in the FPENC during 2015–2020 was higher than the overall linear trend of average annual precipitation during 1960–2020.

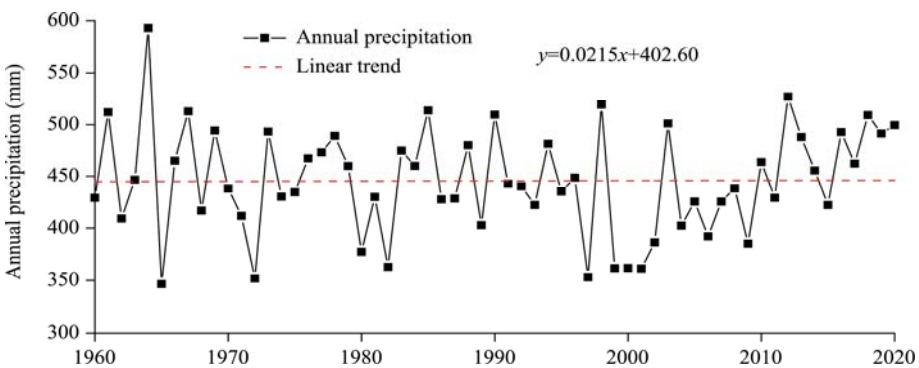

Fig. 2 Annual precipitation change in the farming-pastoral ecotone of northern China (FPENC) from 1960 to 2020

3.2 Temporal variation characteristics of drought and flood based on the SPI

The SPI values calculated for time-scales of 3-months and 12-months (Fig. 3) showed that for the short time-scale (3-months), the variability of dry and wet cycles was high, while for the large time-scale (12-months), the frequency of dry and wet cycles was significantly lower.

The SPI series at the 12-month time-scale (Fig. 3b) indicated that the interannual SPI in the FPENC showed significant fluctuations during 1960–2020, exhibiting an overall non-significant upward trend (P>0.05; increasing rate of 0.02/a). The interannual SPI under a 5-a moving average led to prominent stage characteristics, with obvious turning points in 1972 (downward trend), 1979 (upward trend), 1983 (downward trend), 1988 (upward trend), and 2001 (downward trend). According to Table 1, we divided the interannual SPI into different drought (or flood) grades, and the results showed a noticeable wetting trend in the study area in recent years. There were 16 droughts in the past 61 a, with one drought occurring every 3.81 a on average. The drought periods were mainly concentrated in the periods of 1962–1972, 1980–1982, and 1997–2009, among which severe drought occurred in 1965, 1972, 1982, 1997, 1999, 2000, and 2001. The flood periods in the study area were mainly concentrated in 1961–1967, 1985–2003, and 2012–2020. They reached the severe flood level in 1964 and 2012, consistent with the changes of the annual precipitation in the FPENC. The interannual SPI in the study area showed a downward trend from 1960 to 2012, and disastrous drought frequently occurred during 2000–2012, which is consistent with the research results of Du et al. (2015).

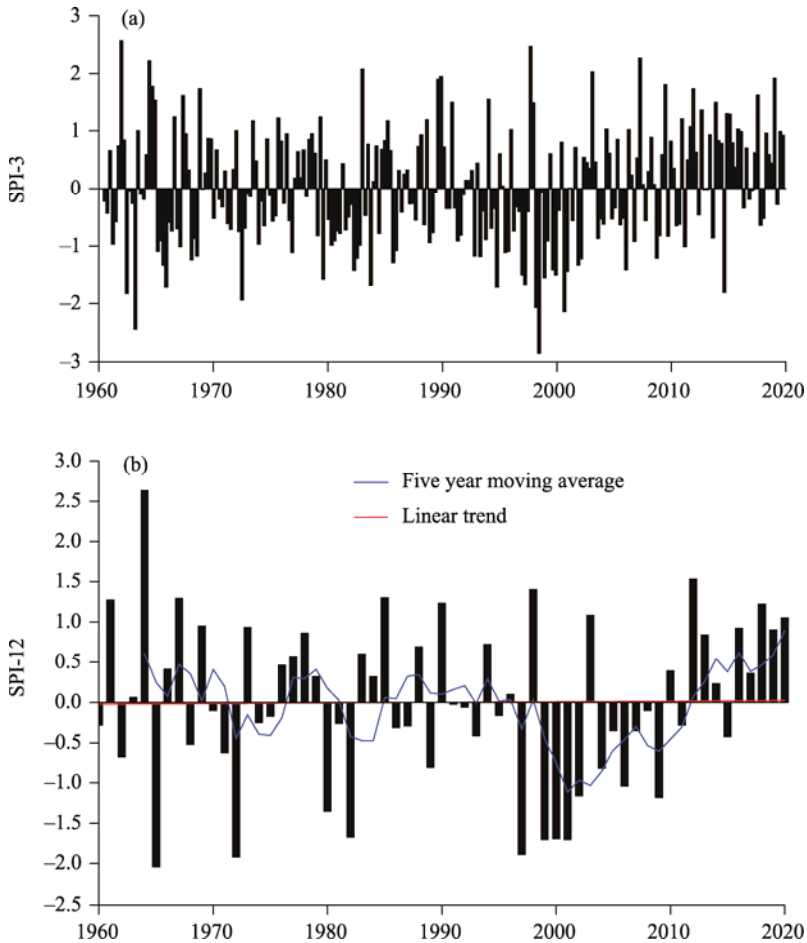

Fig. 3 Standardized Precipitation Index (SPI) values with time-scales of 3-months (SPI-3; a) and 12-months (SPI-12; b) in the FPENC from 1960 to 2020

3.3 Fluctuation characteristics of drought and flood cycles based on the SPI

The isoline of the real part of the wavelet coefficients was plotted (Fig. 4a) to show the periodic changes in the SPI values over different time-scales. The red (blue) color in Figure 4a indicated that the real part of the wavelet coefficient was positive (negative); that is, the precipitation was considerable (slight). The deeper the red (blue) color was, the greater the flood (drought). The SPI value change process showed two kinds of periodic time-scale variation characteristics, namely 2–6 and 9–17 a. The central scale of 9–17 a was 13 a, and the contour map of the wavelet coefficients had a noticeable positive and negative closed center, indicating that the SPI value of the FPENC exhibited a periodic oscillation interval of 13 a. The 2–6 a scale variation was relatively stable between 1960–1979 and 1984–2020, and the cycle change during 1979–1984 was weak. The scale change of 9–17 a was relatively stable during 1997–2017, and the cycle change before 1997 and after 2017 was not remarkable.

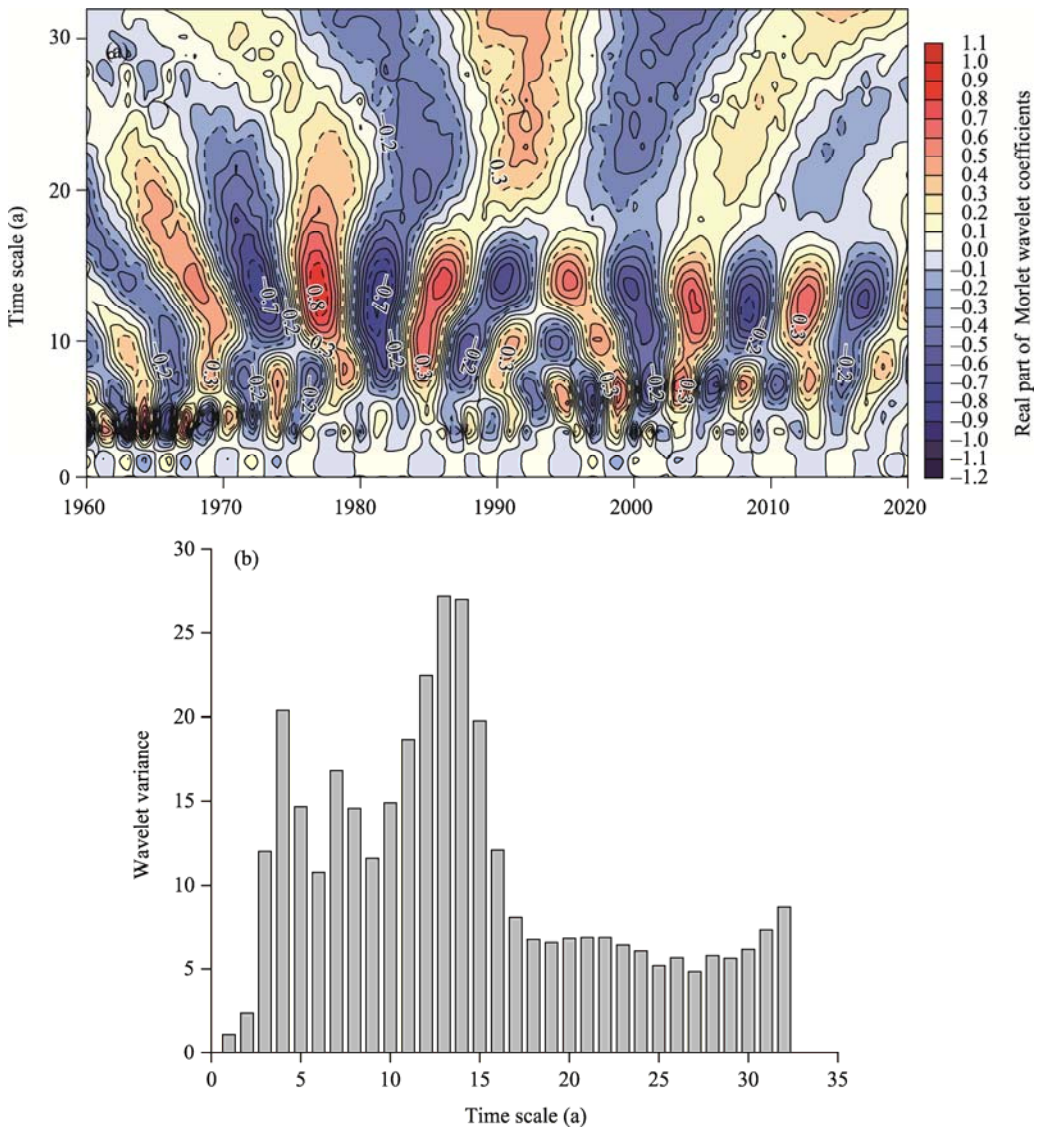

Fig. 4 Isolines of the real part of the Morlet wavelet coefficients (a) and the wavelet variance for the SPI-12 (b) in the FPENC from 1960 to 2020

A wavelet variance diagram can reflect the distribution of the wave energy of the SPI time series with annual scale (Fig. 4b), which can be used to determine the main period of change in the runoff process. It can be seen from the wavelet variance graph that there were three apparent peaks in the isoline of the real part of the Morlet wavelet coefficients based on the SPI index, corresponding to the time-scales of 13, 7, and 4 a, respectively. This result indicated that these three cycles played a significant role in the temporal and spatial changes of drought and flood over the past 61 a. Among them, the maximum peak corresponded to a time-scale of 13 a, indicating that the 13-a cyclical oscillation was the strongest, and that there were alternating cycles between positive and negative values of the SPI, with the most decisive impact on drought and flood in the FPENC, which was the first primary cycle of the SPI value fluctuation. The 4-a time-scale corresponded to the second peak, i.e., the second main period of fluctuation in the SPI value. The 7-a time-scale reached the third peak, with the third main period of the SPI value fluctuation. The fluctuation of the above three cycles controlled the variation of drought and flood characteristics during the entire study period of the FPENC. There were about six alternate periods of drought and flood in 13 a, and the average cycle of drought and flood changes was almost 10 a. There were also 20 alternate periods of drought and flood occurrences in 4 a, and the average cycle of drought and flood changes was about 3 a. About 12 alternate periods of drought and flood existed in 7 a, and the average cycle of drought and flood change was about 5 a. According to the above analysis, the real part of the wavelet coefficients was negative (blue) at time-scales of less than 3 a after 2020, and it can be predicted that there will be a future trend towards drought in the FPENC.

3.4 Spatial variation characteristics of drought and flood based on the SPI

3.4.1 Extents of drought and flood

The drought (or flood) station rate could reflect the evaluation of the extent of drought (or flood) in the FPENC (Fig. 5). The results showed that the percentage of stations recording drought fluctuated between 6.09% and 73.91% during the studied 61 a, with an average value of 31.36%. There were 26 a that the drought station rate was higher than the average value and 35 a that the drought station rate was lower than the average value. The linear trend of the drought extent of the FPENC was described by the red line (Fig. 5) and it showed a downward trend with a decreasing rate of about 0.11/a. This result indicated that the area of the FPENC suffering drought decreased in the recent 61 a. In 1972, the percentage of stations that recorded drought reached its highest value (73.91%) among the studied 61 a in the FPENC, indicating the maximum extent of drought in this year. The percentage of stations that recorded flood fluctuated between 0.86% and 76.52% in the recent 61 a, with an average value of 31.20%. The extent of flood showed an overall upward trend (with an increasing rate of about 0.08/a), indicating that the area of the FPENC suffering flood increased in the studied 61 a.

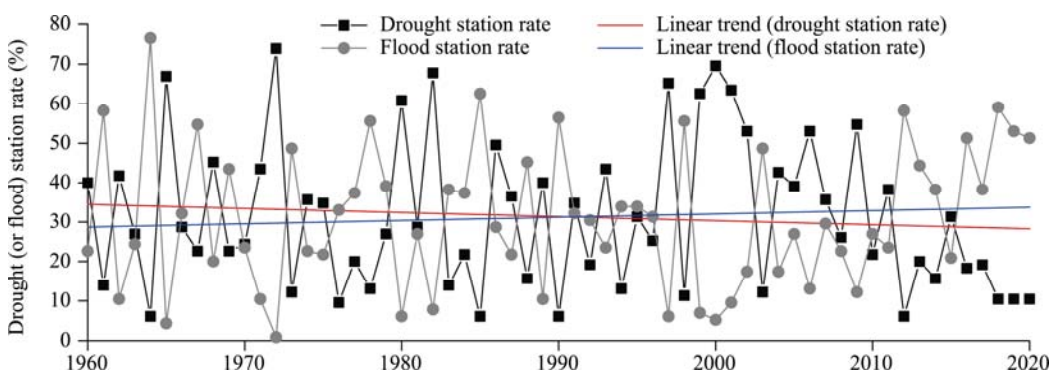

Fig. 5 Change of the drought (or flood) station rate in the FPENC from 1960 to 2020

The frequencies of drought and flood occurrence are summarized in Table 2. From 1960 to 2020, the whole region drought occurred only once (in 1972), and most of the drought occurred in local areas. Regional drought occurred for 3 consecutive years around 2000. In the first 10 a of the 21st century (2000–2009), drought affected the FPENC extensively, with five regional droughts occurring on average once every 2 a. Thereafter, localized drought occurred most frequently, with eight localized droughts from 2010 to 2020 and an average of one drought occurrence every about 1 a. From 1960 to 2020, most of the flood occurred in local areas and partial areas, while few of the flood occurred in regions and the whole region; for example, the whole region flood occurred only once, in 1964.

Table 2 Statistics of drought and flood at different spatial scales in the farming-pastoral ecotone of northern China (FPENC) from 1960 to 2020

Period	No obvious drought	Drought in local areas	Drought in partial areas	Regional drought	Drought event of the whole region
1960–1969	1	5	3	1	0
1970–1979	1	5	3	0	1
1980–1989	1	4	3	2	0
1990–1999	1	4	3	2	0
2000–2009	0	2	3	5	0
2010–2020	1	8	2	0	0
Period	No obvious flood	Flood in local areas	Flood in partial areas	Regional flood	Flood event of the whole region
1960–1969	1	4	2	2	1
1970–1979	1	4	4	1	0
1980–1989	2	4	3	1	0
1990–1999	2	1	5	2	0
2000–2009	2	7	1	0	0
2010–2020	0	3	3	5	0

3.4.2 Spatial distribution characteristics of drought and flood grades

Figure 6 shows the spatial distribution of drought and flood grades in the FPENC. In 1960, severe drought and flood rarely occurred in the study area (Fig. 6a). Dry regions were distributed in the eastern part of the northwestern segment, in the central part of the northern segment, and at the junction of the northern and northeastern segments in the FPENC. Most of these parts had light drought, with moderate and severe drought concentrated in Gansu Province and Inner Mongolia Autonomous Region. Flooded areas were focused on the northeast of the northeastern segment. In 1970, drought and flood disasters were relatively few in the study area, with no drought or flood occurring in most regions (Fig. 6b). Flood was mainly concentrated in Gansu Province and was mainly light flood. Light drought mostly occurred in the northern segment, while moderate drought occurred in Heilongjiang and Shaanxi provinces. In 1980, most regions of the study area occurred drought except Heilongjiang Province (Fig. 6c). Regions of moderate and severe drought were concentrated in the northern part of the northwestern segment, the eastern part of the northern segment, and the western part of the northeastern segment. In 1990, flood occurred more frequently in the study area as a whole and was concentrated in the central part of the northwestern segment, and most of the regions from the northern segment to the northeastern segment (Fig. 6d). Flood occurred mainly in light or moderate grade, and drought was only distributed in the northwest of Qinghai Province. In 2000, the entire study area was normal with drought only in partial areas; light drought was concentrated in the northwestern segment and in the eastern part of the northern segment, while moderate and severe drought occurred in the northeast part of the northwestern segment, the eastern part of the northern segment, and the most

areas of the northeastern segment, except Jilin Province (Fig. 6e). In 2010, most parts of the study area exhibited normal conditions. Drought mainly occurred in Gansu Province and was mostly light, while flood was concentrated in Hebei and Liaoning provinces (Fig. 6f). In 2020, drought was rare in the study area, and most of drought occurred in the southwest of Liaoning Province (Fig. 6g). Light flood mainly happened in the northwestern and northern segments, with the most remarkable occurrence in the northwestern segment being in the south of Gansu Province. In most regions of the northern segment, flood was light or moderate. In the northeastern segment, the degree of flood increased from west to east.

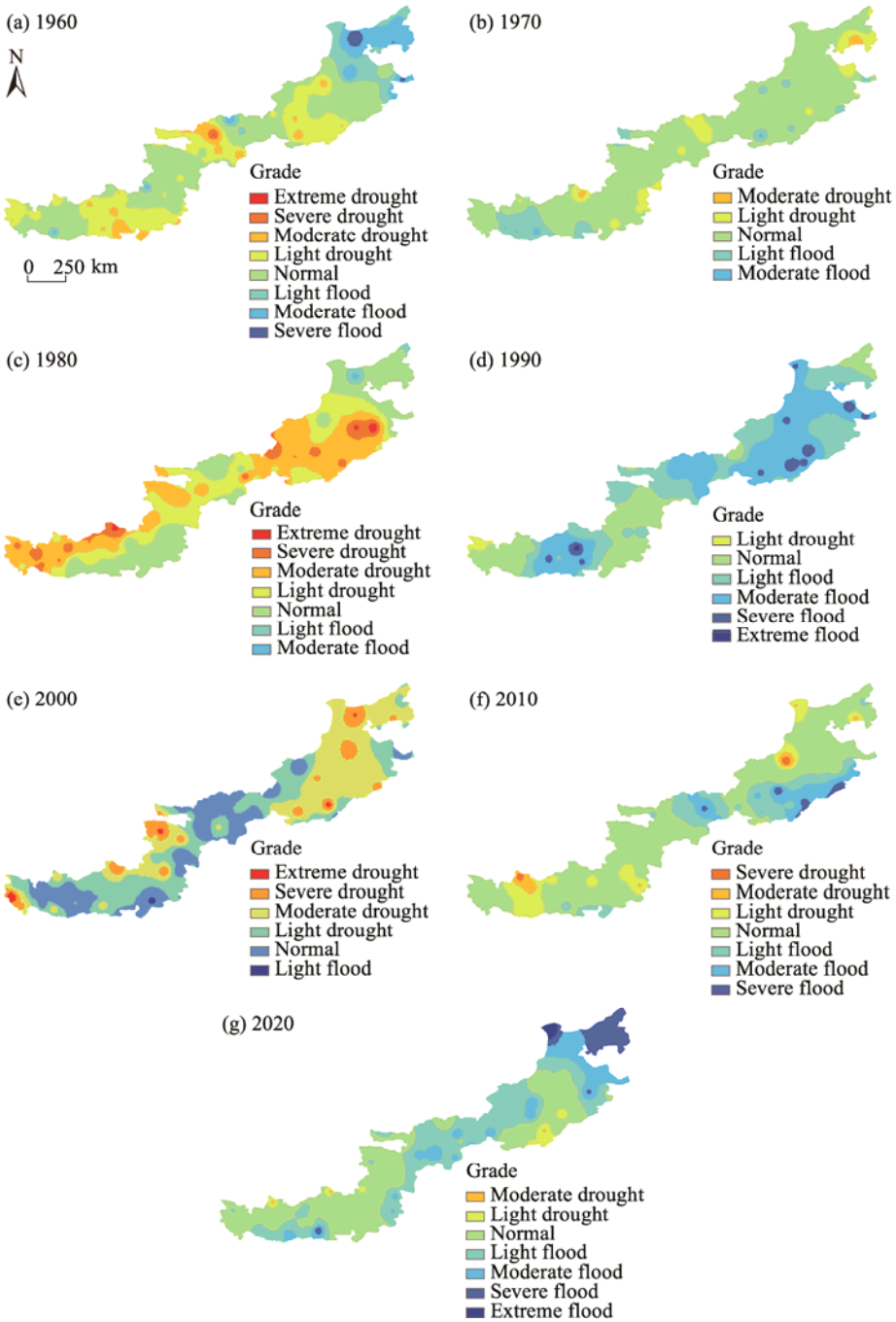

Fig. 6 Spatial distribution characteristics of drought and flood grades in the FPENC in 1960 (a), 1970 (b), 1980 (c), 1990 (d), 2000 (e), 2010 (f), and 2020 (g)

3.5 Spatial variations of drought and flood frequencies based on the SPI

As can be seen from the total drought frequency (Fig. 7a), the drought frequency was relatively high at about 33%–42% in most regions of Gansu Province and Ningxia Hui Autonomous Region in the northwestern segment, and in Liaoning and Heilongjiang provinces in the northeastern segment. The drought frequency was lower at 24%–33% in Qinghai and Shaanxi provinces in the northwestern and northern segments, except in parts of Hebei Province and most regions in the northeastern segment. According to the spatial distribution frequency map shown in Figure 7b, the frequency of light drought was lower (13%–28%) in most regions of the northwestern segment, the eastern part of the northern segment, and Heilongjiang and Liaoning provinces in the northeastern segment. Light drought occurred at low frequency in the central region of the northern segment. It was relatively low at about 4%–13% in the southeastern parts of Inner Mongolia Autonomous Region and Jilin Province in the northeastern segment. The frequency distribution for moderate drought (Fig. 7c) showed that the frequency was higher in the eastern part of the northwestern segment (at about 8%–22%) and much lower in the western part, at 3%–8%. In the northern segment, low frequency of moderate drought was concentrated in Shanxi and Hebei provinces, while the other regions had high frequency of moderate drought. In the northeastern segment, high frequency of moderate drought was concentrated in Liaoning and Heilongjiang provinces, as well as the parts of Inner Mongolia Autonomous Region near Liaoning Province. The overall frequency of severe drought (Fig. 7d) was less than 10%. At the frequency range of 3%–10%, the values were higher in Qinghai and Gansu provinces in the western part of northwestern segment, Shanxi and Hebei provinces in the central part of the northern segment, and most regions in the northeastern segment, except Jilin Province. The frequency of severe drought in Shaanxi Province and other areas was less than 3%. The spatial distribution map of extreme drought frequency (Fig. 7e) showed a probability of occurrence below 7%. The frequency of extreme drought was relatively high at 1%–7% in Shaanxi Province in the northwestern segment, the most regions of the northern segment, and the eastern part of the northeastern segment. The frequency of extreme drought in other regions was lower than 1%.

The flood frequency was relatively high, with values of 30%–37% in most regions of Qinghai Province in the northwestern segment, Inner Mongolia Autonomous Region and Hebei Province in the northern segment, and Liaoning and Heilongjiang provinces in the northeastern segment (Fig. 7f). The values of flood frequency in other regions were 22%–30%. According to the spatial distribution map of light flood frequency (Fig. 7g), the frequency of light flood was relatively high, at 15%–24% in Qinghai and Gansu provinces in the northwestern segment and in the northern segment except partial regions of Shanxi Province. The flood frequency was low (4%–15%) in Ningxia Hui Autonomous Region and Shaanxi Province in the northwestern segment and most regions in the northeastern segment. For moderate flood, the regions with low frequency of moderate flood (1%–10%) were concentrated in Qinghai Province in the northwestern segment and the western part of the northern segment. The regions with high frequency of moderate flood in the northeastern segment were concentrated in Inner Mongolia Autonomous Region (Fig. 7h). The frequency of severe flood was less than 10%, as shown in Figure 7i. The frequency of severe flood was higher in the eastern part of Gansu Province in the northwestern segment, the western part of the northern segment, and most regions in the northeastern segment, with values of 5%–9%. As can be seen from the spatial distribution map of the extreme flood frequency (Fig. 7j), the occurrence probability of extreme flood was below 7%. The frequency of extreme flood was relatively high in most regions of the northwestern segment, the western part of the northern segment, and Inner Mongolia Autonomous Region in the northeastern segment, at 1%–6%; the frequency of extreme flood in the other regions of the FPENC was lower than 1%.

4 Discussion

4.1 Applicability of the SPI analysis

Precipitation is readily available in basic climatic data. It varies on both temporal and spatial scales, playing an essential role in predicting seasonal and interannual regional climate (Chen et al.,

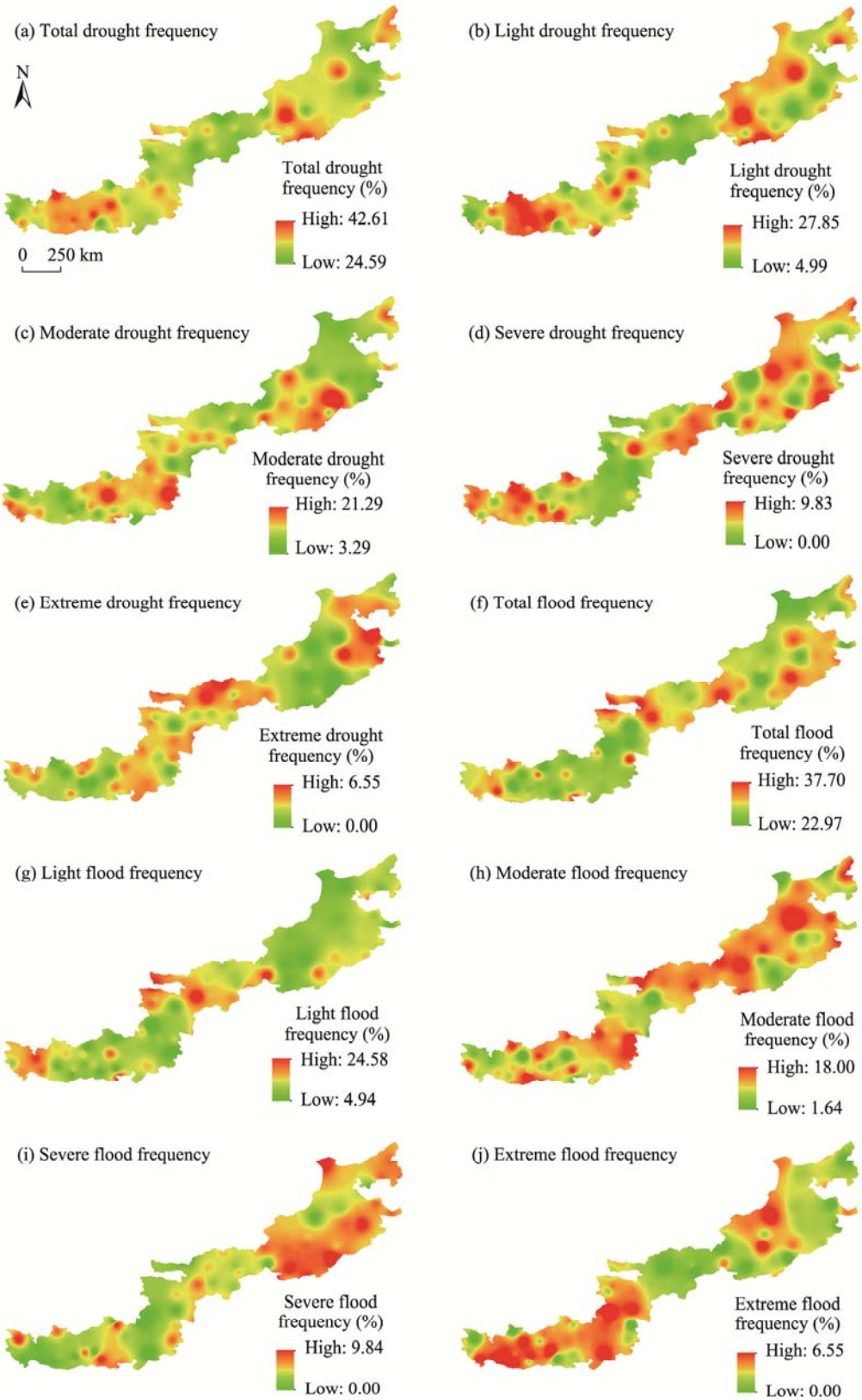

Fig. 7 Spatial distribution of drought (a–e) and flood (f–j) frequency in the FPENC

2009). At present, many indices are used to evaluate drought and flood disasters, including the SPI, Z index, PDSI, and SPEI. The SPI is based on precipitation data and assumes that the regional precipitation follows a skewed probability distribution function. The advantages of the SPI are: (1) it can be used on different time-scales, such as 1 month, 3 months, and 12 months; (2) it reflects the severity of drought and flood in different periods and regions; and (3) its calculation is relatively simple and requires fewer data.

Therefore, the SPI is widely used in drought and flood monitoring and climate assessment in various regions (Wang et al., 2015; Gou et al., 2019; Yu et al., 2019; Elouissi et al., 2021; Li et al., 2021). This paper combined the SPI with GIS spatial interpolation to analyze the drought and flood characteristics and the temporal and spatial changes in the FPENC over the past 61 a. This study found that the interannual SPI in the study area followed a downtrend before 2012, showing a noticeable tendency towards aridity. After 2012, the interannual SPI in the study area followed an upward trend and exhibited a noticeable tendency towards humidification. Disastrous drought frequently occurred in the 2010s. During the past 61 a, drought occurred frequently in the northwestern part of the FPENC. The degree of drought in the northern and northeastern segments was more serious, which is basically consistent with the conclusions of the published literatures (Du et al., 2015; Teng and Feng, 2021).

4.2 Spatio-temporal variations of drought and flood based on the SPI

In this paper, the temporal and spatial variations of the SPI in the FPENC could only be proved with the addition of some data taken from the literature. Therefore, it is necessary to further analyze the temporal and spatial variation characteristics of the SPI and verify the theoretical results according to the observed drought and flood conditions, so as to reflect the actual drought and flood characteristics in this region more accurately. This study showed that in 1960, drought occurred mainly in the eastern part of the northwestern segment and the central part of the northern segment, as well as at the junction of the northern and northeastern segments of the FPENC (Fig. 6a–e). In 1970, there were fewer drought and flood, and light drought was more frequent in the northern segment. In 1980, drought occurred in all provinces except Heilongjiang Province, and the regions with moderate and severe drought was concentrated in the northern part of the northwestern segment, the eastern part of the northern segment, and the western part of the northeastern segment. In 1990, flood was more frequent over the entire study area and concentrated in the middle part of the northwestern segment and most regions of the northern segment to the northeastern segment. In 2000, the northeastern part of the northwestern segment, the eastern part of the northern segment, and the northeastern segment (except in most parts of Jilin Province) suffered moderate and severe drought.

The historical drought recorded in the China Meteorological Disasters Statistics (Comprehensive Volume) (Ding, 2008) showed a serious drought in northern China in winter and spring of 1960. The whole Gansu Province suffered a severe drought, and the drought in Inner Mongolia Autonomous Region was extensive and prolonged. Drought occurred in autumn and early winter of 1970 in North China, due to very little rainfall and snowfall. In 1980, the prolonged and severe drought affected a wide area of Gansu Province. From the autumn of 1979 to the end of August 1980, there was no rainfall in Ningxia Hui Autonomous Region, and drought was most serious in Hebei Province. The Luanhe River, Weihe River, and Chaobai River retained low water flow, while other river channels dried up. In the farming and pastoral areas of Inner Mongolia Autonomous Region, there had been little rainfall for a long time and the groundwater level had generally dropped by more than 1.0 m. In Liaoning Province, there was little rainfall after summer, and drought occurred in most regions. In 1990, rainstorm and flood affected some regions, and heavy rainfall occurred in the eastern part of the northwestern segment, most parts of the northern segment, and the southern part of the northeastern segment. Some regions did experience successive rainfall with high intensity. In spring and summer of 2000, there was a serious drought in the northern segment. Precipitation in most regions north of the Yangtze River

was low, causing a widespread spring drought in the northwestern segment, the northern segment, and the northeastern segment. In summer, precipitation in the northern segment, the eastern part of the northwestern segment, and the northeastern segment were even lower, and there was drought in spring and summer, quite severe in some regions.

By comparing the historical drought and flood recorded in the China Meteorological Disasters Statistics (Comprehensive Volume) (Ding, 2008), it was found that in some regions, our analysis of drought and flood characteristics in the FPENC based on the SPI was slightly different from the actual situation. However, in most regions, the results of this study were consistent with the historical drought and flood records. Therefore, the SPI can provide robust characterization of drought and flood characteristics in the FPENC.

5 Conclusions

Based on the analysis of the temporal characteristics, periodic features, and spatial patterns of drought and flood in the FPENC from 1960 to 2020, the following conclusions can be drawn. The annual precipitation in the FPENC first decreased and then increased over the last 61 a. Overall, the interannual SPI in the FPENC showed a slight upward trend (P>0.05), and the wetting trend in the study area was evident in recent years, consistent with the changes in annual precipitation. The Morlet wavelet transform results showed that drought and flood disasters had periodic variation characteristics of 2–6 and 9–17 a, and drought and flood disasters occurred alternately. After 2020, the FPENC will probably suffer drought. In the past 61 a, the extent of drought in the FPENC has reduced. Drought and flood disasters occurred only once in the whole region but frequently in some regions. The temporal and spatial distribution of the degree and frequency of drought and flood in the FPENC showed regional differences. Therefore, this study provides a theoretical basis for the management of the drought and flood disasters and future policy-making in the FPENC.

Acknowledgements

This study was financially supported by the National Natural Science Foundation of China (41871097).

References

Anandharuban P, Elango L. 2021. Spatio-temporal analysis of rainfall, meteorological drought and response from a water supply reservoir in the megacity of Chennai, India. Journal of Earth System Science, 130(1): 1–20.

Cao Y Q, Ning Y, Li L H, et al. 2021. Analysis of the characteristics of drought and flood in Hebei Province based on SPEI index. Journal of North China University of Water Resources and Electric Power (Natural Science Edition), 42(3): 76–85. (in Chinese)

Chen L J, Chen D L, Wang H J, et al. 2009. Regionalization of precipitation regimes in China. Atmospheric and Oceanic Science Letters, 2(5): 301–307.

China Meteorological Administration. 2006. Classification of Meteorological Drought (GB/T 20481-2006). Beijing: Standards Press of China, 14–15. (in Chinese)

Ding Y H. 2008. China Meteorological Disasters Statistics: Comprehensive Volume. In: Wen K Q. China Meteorological Disasters Statistics. Beijing: Meteorological Press, 120–227. (in Chinese)

Du H M, Yan J P, Wang P T. 2015. The drought disaster and its response to the warming-drying climate in the farming-pastoral ecotones in northern China. Journal of Arid Land Resources and Environment, 29(1): 124–128. (in Chinese)

Elouissi A, Benzater B, Dabanli I, et al. 2021. Drought investigation and trend assessment in Macta watershed (Algeria) by SPI and ITA methodology. Arabian Journal of Geosciences, 14(14): 1–13.

Fang Z H, He C Y, Liu Z F, et al. 2020. Climate change and future trends in the Agro-Pastoral Transitional Zone in Northern China: The comprehensive analysis with the historical observation and the model simulation. Journal of Natural Resources, 35(2): 358–370. (in Chinese)

Gao C, Zhang X, Lu M, et al. 2016. Advances in threshold of meteorological flood and drought inducing factors in agriculture. Journal of Irrigation and Drainage, 35(11): 111–116. (in Chinese)

Gao S Q, Duan R, Wang H S, et al. 2021. Farming-pastoral ecotone of northern China plays important role in ensuing national

food security. Bulletin of Chinese Academy of Sciences, 36(6): 643–651. (in Chinese)

Gou F Z, Qiang W B, Cheng Y T. 2019. Analysis of multi-scale drought characteristics in Wei River Basin based on SPI. Journal of Xi'an University of Technology, 35(4): 443–451. (in Chinese)

Hu T Y, Zhu J Y, Xiang J X, et al. 2020. The method of contour generation using measurement date based on IDW interpolation. Port & Waterway Engineering, (7): 199–205. (in Chinese)

Kalisa W, Zhang J, Igbawua T, et al. 2020. Spatio-temporal analysis of drought and return periods over the East African region using Standardized Precipitation Index from 1920 to 2016. Agricultural Water Management, 237: 106195, doi: 10.1016/j.agwat.2020.106195.

Li M M, Yan J P, Ding C X. 2014. Climate change and response characteristics of drought and flood in farming-pastoral ecotone of northern China. Bulletin of Soil and Water Conservation, 34(5): 304–308. (in Chinese)

Li S P, Li X H, Zeng S L, et al. 2021. Analysis of drought and flood variation characteristics in northern Guangdong based on SPI index. Guangdong Meteorology, 43(3): 1–5. (in Chinese)

Li X L, Yang L X, Tian W, et al. 2018. Land use and land cover change in agro-pastoral ecotone in Northern China: A review. Chinese Journal of Applied Ecology, 29(10): 3487–3495. (in Chinese)

Liu Z J, Liu Y S, Li Y R. 2018. Anthropogenic contributions dominate trends of vegetation cover change over the farming-pastoral ecotone of northern China. Ecological Indicators, 95: 370–378.

Salehnia N, Salehnia N, Torshizi A S, et al. 2020. Rainfed wheat (*Triticum aestivum* L.) yield prediction using economical, meteorological, and drought indicators through pooled panel data and statistical downscaling. Ecological indicators, 111: 105991, doi: 10.1016/j.ecolind.2019.105991.

Shahabfar A, Eitzinger J. 2013. Spatio-temporal analysis of droughts in semi-arid regions by using meteorological drought indices. Atmosphere, 4(2): 94–112.

Teng H Y, Feng K P. 2021. Spatio-temporal distribution of drought in Northwest China based on SPEI drought Index. Agriculture and Technology, 41(8): 887–893. (in Chinese)

Teolis A. 1998. Computational signal processing with wavelets. Boston, MA: Birkhauser, 62–65.

Wang W, Zhu Y, Xu R G, et al. 2015. Drought severity change in China during 1961–2012 indicated by SPI and SPEI. Natural Hazards, 75(3): 2437–2451.

Wu H, Hayes M J, Weiss A, et al. 2001. An evaluation of the Standardized Precipitation Index, the China-Z Index and the statistical Z-Score. International Journal of Climatology, 21(6): 745–758.

Xu D H, Zhang Q, Huang H P. 2020. Application of the combined ARIMA-SVR model in drought prediction based on the Standardized Precipitation Index. Agricultural Research in Arid Areas, 38(2): 276–282. (in Chinese)

Yang J H, Jiang Z H, Wang P X, et al. 2008. Temporal and spatial characteristic of extreme precipitation event in China. Climatic and Environmental Research, 13(1): 75–83. (in Chinese)

Yu J R, Ai P, Yuan D B, et al. 2019. Spatial-temporal characteristics of drought in Heilongjiang Province based on standardized precipitation index. Arid Land Geography, 42(5): 1059–1068. (in Chinese)

Zhang Q F, Liu G X, Yu H B, et al. 2015. Analysis of drought characteristics in Xilingol League based on standardized precipitation index. Journal of Natural Disasters, 24(5): 119–128. (in Chinese)

Zhou H, Zhou W, Liu Y B, et al. 2019. Meteorological drought migration in the Poyang Lake Basin, China: switching among different climate modes. Journal of Hydrometeorology, 21(3): 415–431.